Title: FORCCHN V2.0: An individual-based model for predicting multiscale forest carbon dynamics

Authors: Jing Fang[1,2], Herman H. Shugart[3], Feng Liu[1,2], Xiaodong Yan[4*], Yunkun Song[4], and Fucheng Lv[4]

1. CAS Key Laboratory of Aquatic Botany and Watershed Ecology, Wuhan Botanical Garden, Chinese Academy of Sciences, Wuhan 430074, China

2. Center of Plant Ecology, Core Botanical Gardens, Chinese Academy of Sciences, Wuhan 430074, China

3. Department of Environmental Sciences, University of Virginia, Charlottesville, VA 22904, USA.

4. State Key Laboratory of Earth Surface Processes and Resource Ecology, Beijing Normal University, Beijing 100875, China

Corresponding author: Xiaodong Yan (yxd@bnu.edu.cn)

Abstract

Process-based ecological models are essential tools to quantify and predict forest growth and carbon cycle under the background of climate change. The accurate description of phenology and tree growth processes enables an improved understanding and predictive modeling of forest dynamics. An individual tree-based carbon model, FORCCHN2 (FORest ecosystem Carbon budget model for CHiNa Version 2.0), used the non-structural carbohydrates (NSC) pools to couple tree growth and phenology. This model performed well in reducing uncertainty in predicting forest carbon fluxes. Here, we describe the framework in detail and provide the source code of FORCCHN2. We also present a Dynamic Link Library (DLL) package containing the latest version of the FORCCHN2 model. This package has the advantage of using Fortran as an interface to make the model runs fast on a daily step, the package also allows the users to call it with their preferred computer tools (e.g., Matlab, R, Python, *etc.*). FORCCHN2 model can be used directly to predict the spring and autumn phenological dates as well as the daily carbon fluxes (including photosynthesis, above- and belowground autotrophic respiration, and soil heterotrophic respiration) and biomass on plot, regional, and hemispheric scales. As case studies, we provide an example of the FORCCHN2 running, model validations in 78 forest sites, and an example model application for the carbon dynamics of Northern Hemisphere forests. We demonstrate the FORCCHN2 model can produce a reasonable agreement with flux observations. Given the potential importance of the application of this ecological model in many studies, there is substantial scope for using the FORCCHN2 model in fields as

19   diverse as forest ecology, climate change, and carbon estimations.

21   **Keywords:** ecological models, forest ecosystems, carbon cycle, non-structural carbohydrates, individual

22   tree, leaf phenology

1. Introduction

Forests contribute an enormous carbon flux to terrestrial ecosystems (Pan et al. 2011, Keenan and Williams 2018). Thus, accurate estimation and prediction of forest dynamics play an important role in understanding the carbon cycle in the background of global change (Beer et al. 2010, Harris et al. 2021). Over past decades, process-based ecological models have often been considered as effective tools for evaluating forest dynamics at multiple scales (Friedlingstein et al. 2020).

Even though the ecological models are widely used in the prediction of forest dynamics, large uncertainties remain (Huntzinger et al. 2012, Friedlingstein et al. 2020). Some of these uncertainties can be attributed to the lack of effective phenological parameterization in the models and the neglect of autumn phenology modeling (Raczka et al. 2013), both of which need to be based on an improved understanding and coupling of mechanisms regulating forest phenology (Piao et al. 2019). Furthermore, the previous models assumed that the reserve carbon of trees acts merely as a carbon buffer pool between sink and source (Schiestl-Aalto et al. 2015). Recent studies considered the stored carbon as the non-structural carbohydrates (NSC), which may have an active role on tree growth and carbon dynamics (Martínez-Vilalta et al. 2016, Piper 2020). For example, trees rely on NSC to resume growth after the non-growing season (Furze et al. 2019). The individual tree-based model, FORCCHN version 2.0 (FORCCHN2), has been developed to treat these considerations by integrating two NSC pools (NSC active and slow pool) and optimizing phenological parameters (Fang et al. 2020a, Fang et al. 2021).

FORCCHN2 has improved performance for predicting forest carbon sinks compared to other models in North American forests (Fang et al. 2020b).

This model provides the temporal predictions of individual tree growth processes as well as the spatially explicit estimations of carbon dynamics on biomass, photosynthesis, autotrophic respiration, and heterotrophic respiration (Fang et al. 2020b). The latest version can capture forest carbon dynamics, but current runs of FORCCHN2 have limitations that prevent a seamless integration of the model into the data-oriented software environment (e.g., Matlab, R, Python, etc.). FORCCHN2 and its previous versions are designed originally for the daily calculation of individual trees in a given plot and implemented in Fortran (Ma et al. 2017, Zhao et al. 2019, Fang et al. 2020a). Fortran ensures the calculation efficiency and shortens the model runtime, but the model code and the implementation are not designed for the end-users with appropriate help and instruction files. Moreover, until now, the FORCCHN2 model has only been validated and applied in North America, and there has been no comprehensive publication describing the model itself and no hemispheric-scale validation using this model.

Here, we present a DLL package aimed to provide a flexible and user-friendly interface for implementing the newest FORCCHN2 model. Meanwhile, we provide the source code and the detailed description of this model and demonstrates that FORCCHN2 model can predict a realistic and stable carbon dynamics in the hemispheric-scale forests. With the package, users can conveniently run model predictions on the individual, plot, regional, continental, and hemispheric scales according to their

59 computer tools. This package is compiled by Fortran 95 and thus can keep the high calculation efficiency.

60 We also demonstrate the functionality and example of FORCCHN2 model, perform the model validation

61 at the carbon flux sites, apply the model on a hemispheric scale (i.e. Northern Hemisphere), and provide

62 an open-access dataset of carbon outputs across the Northern Hemisphere.

63

2. FORCCHN2 description

65 FORCCHN2, an individual tree-based carbon dynamic model, predicts the daily processes of NSC,

66 photosynthesis, growth, phenophase, vegetation (autotrophic) respiration, and soil dynamics in forests

67 (**Fig. 1** and **Method S1-S2**). This model is driven by the daily climate data and uses the leaf area index

68 (LAI) to initialize the vegetation information (i.e., trees' number, DBH, height, and biomass) on a fixed

69 area (**Method S3**).

70 For an individual tree, the NSC produced by photosynthesis is considered as the substrate supply for

71 vital activities, such as participating in the autotrophic respiration and forming the structural carbon pools

72 (i.e., leaves, wood, and fine roots) through growth (Sala et al. 2012, Richardson et al. 2013). The NSC

73 production is limited by external environmental factors (e.g., water, temperature, CO_2, etc.), and the NSC

74 consumption for the growth of each structural carbon pool (i.e., leaves, wood, and fine roots) is regulated

75 by phenology factors and daily climate (Schiestl-Aalto et al. 2015, Delpierre et al. 2019). The phenophase

76 of spring and autumn in FORCCHN2 is controlled by heat and chilling requirements, respectively (Fang

77 et al. 2022). The spring phenophase is decided by the effective temperature with the Thermal Time model

78 (**Eqn 39-40**), and the autumn phenophase is decided by the effective temperature and photoperiod with

79 the Cold Degree-Day model (**Eqn 41-42**). The model divides NSC into an active NSC pool and a slow

80 NSC pool. The active pool provides the essential NSC consumption for daily activities; the slow pool is

81 an NSC storage pool providing the necessary NSC for requirements when the contemporaneous active

82 pool is insufficient, such as maintaining vegetation respiration during the non- and early-growing seasons.

83 These NSC pools allow trees to be dead if the NSC storage drops below zero.

84   Dynamic changes of NSC production, allocation and consumption drive change in the NSC active

85 pool (NSC_{active}, kg C) at a daily time step. The NSC slow pool (NSC_{slow}, kg C) is defined as the NSC

86 storage pool. The changes in the daily active pool and yearly slow pool are:

$$\frac{dNSC_{active}}{dt} = \frac{dGPP}{dt} - \sum \frac{dR_j}{dt} - \sum \frac{dR_j^G}{dt} - \sum \frac{dG_j}{dt} \tag{1}$$

$$NSC_{slow}(y) = NSC_{active,y} \tag{2}$$

87 Where t is the day of the year; y is the yth year; j is each part of the tree (i.e. leaf, fine roots, and wood);

88 GPP is gross primary productivity (kg C); R is the maintenance respiration (kg C); R^G is the growth

89 respiration (kg C); G is the carbon demand of growth (kg C); $NSC_{active,y}$ is the size of NSC active pool at

90 the end of yth year (kg C). The NSC active pool is initialized to zero on the first day of the next year. The

91 calculation of GPP, maintenance respiration, growth respiration, and growth processes can be found in

92 **Method S1** and **S2**.

For the relationship between an individual tree with its neighbors, the model uses a distance-independent gap model to describe the light competition. To simplify the physiological and ecological parameters, each individual tree is assumed to belong to the plant functional types (PFTs) instead of specific tree species (**Table S2**). The PFT of one tree is decided by tree species when using the inventory data or it is estimated by forest types and random function when using the satellite data. The phenological parameters are parameterized by the local climate and observed phenological time in the first year (**Eqn S43-S45**). A part of structural carbon pools is then transferred into the soil pools by litter-fall. The main soil processes in the FORCCHN2 model are soil organic matter (SOM) decomposition, N mineralization, and water dynamics. According to the attribute, soil pools include above- and belowground metabolic and structural pools; fine and coarse woody litter pools; active, slow, and resistant SOM pools (**Table S4**). Except for these pools, the soil nitrogen pool also includes the inorganic nitrogen pool.

After each time step, the predicted vegetation and soil statements are converted into output variables such as biomass and carbon fluxes. The carbon fluxes of plot scale include GPP (kg C m^{-2}), net primary productivity (NPP, kg C m^{-2}), and net ecosystem productivity (NEP, kg C m^{-2}). The NPP of a given plot at the daily step is determined by the GPP, R (kg C m^{-2}), R^G (kg C m^{-2}). The NEP of a given plot at the daily step is determined by the GPP, R, R^G, and soil respiration (R$_S$, kg C m^{-2}):

$$\frac{dNPP}{dt} = \sum \frac{dGPP_n}{dt} - \sum \frac{dR_n}{dt} - \sum \frac{dR_n^G}{dt} \tag{3}$$

$$\frac{dNEP}{dt} = \frac{dNPP}{dt} - \frac{dR_S}{dt} \tag{4}$$

109   Where *n* is the *n*th tree of the plot.

110   The more detailed description, including inputs, outputs, calculation processes, and parameter sets

111   of FORCCHN2, can be found in **Table 1**, **Method S1-S3**, and **Table S2-S5**.

112

113   **3.   Example runs**

114   Here, we provide an integrated DLL package ('FORCCHN2.dll') to simplify the usage of the

115   FORCCHN2 model. This file is highly flexible and it allows users to adapt model runs to their own

116   computer language (e.g., Matlab, R, Fortran, Python, etc.). Except for the model inputs, using only one

117   command can call the calculation of the model. We provide users with 32- and 64-bit DLL packages to

118   choose the most suitable version.

119   We take the Harvard Forest (a deciduous broadleaf forest in the eastern United States) and use Matlab

120   as an example run to demonstrate the functionality of the FORCCHN2 model (the code of example also

121   can be accessed via https://github.com/JingF1/FORCCHN2_model.git). First, we install and load the

122   package:

123   >>name1=('XXX');%load path of the FORCCHN2 DLL package

124   >>name2=[name1,'FORCCHN2_64.dll']; %input 64-bit or 32-bit DLL file

125   >>name3=[name1,'FORCCHN2.h'];%input header file

126   >>loadlibrary(name2,name3);%load the DLL package

127   Then, we input the data of Harvard Forest during 1991-2012. The inputs include the year information,

128   the initialization data (i.e., geography, vegetation, and soil data), and the driven data (i.e., climate data).

129   The more detailed information and format of these input data can be found in the example code

130   ('FORCCHN2_run_example.m').

131   After inputting all data, we predict the dynamics of this forest for a period of 22 years. We can choose

132   four output results of the FORCCHN2:

133   >>[fj,yxc,dayout,yearout]=calllib('FORCCHN2_64','forcchn2',fj,yxc,dayout,yearout,ntrees,ny0,ny,nday

134   s,lat,lon,ele,tmax,tmin,tmean,pho,prec,ra,rh,wind,sfc,pwp,vw,sc0,sn0,silt,sand,class1,evergr0,deci0,lai0,

135   co2);% run model with DLL file

136   >>unloadlibrary FORCCHN2; %unload the DLL package

137   Where the four outputs include: 'fj' is the phenology dates, which included the start time of leaf

138   growth (SOS) and the end time of leaf growth (EOS); 'yxc' is the allocation parameter of each soil pool,

139   which can be used as input instead of the initial soil allocation parameters; 'dayout' is the daily carbon

140   dynamics, which included above- and belowground biomass, gross primary productivity (GPP), above-

141   and belowground respiration, soil heterotrophic respiration, litter-fall biomass, and soil carbon; 'yearout'

142   is the yearly carbon dynamics.

143

144   **4. External validation**

145 The comparison between model simulations and external observations is considered as the rigorous model

146 test (Houlahan et al. 2017). Among the various observation methods, the eddy-covariance (EC) technique

147 can provide high-frequency and accurate measurements of relevant data (Keenan and Williams 2018).

148 The FLUXNET2015 dataset (Pastorello et al. 2020, https://fluxnet.org/) from the EC tower is an ideal

149 dataset to validate the FORCCHN2 model in predicting carbon flux dynamics. This dataset is developed

150 by using the EC (Eddy Correlation) technique to measure the net ecosystem CO_2 exchange (NEE, which

151 equaled to the negative of NEP) directly in the footprint of the EC tower. The Variable Ustar Threshold

152 (VUT) Mean values of FLUXNET2015 are used in this work. We extracted the flux data from the mean

153 value of the nighttime and the daytime method. The nighttime method uses nighttime NEE data to

154 parameterize a respiration-temperature model that is then applied to the whole dataset to estimate

155 Ecosystem Respiration (ER). The vegetation GPP is then calculated as the difference between ER and

156 NEE (Lasslop et al. 2010). The daytime method uses daytime and nighttime NEE data to parameterize a

157 model with one component based on a light-response curve and vapor pressure deficit for GPP, and a

158 second component using a respiration-temperature relationship similar to the nighttime method

159 (Pastorello et al. 2020). Due to the different phenological phasing in the Northern and Southern

160 Hemisphere, our predictions focus on the Northern Hemisphere. We chose the 78 active forest sites with

161 continuous daily observations in the Northern Hemisphere (i.e., a total of 232664 observations). These

162 sites cover the most forest types, including the evergreen broadleaf forest (EBF), evergreen needleleaf

forest (ENF), deciduous broadleaf forest (DBF), and mixed forest (MF). The distribution and information

of all sites are shown in **Fig. S1** and **Table S1**. We also extract the climate data from the FLUXNET2015

dataset to drive the model. Soil data are taken from the Harmonized World Soil Database (HWSD) V1.2

(http://www.fao.org/soils-porta l/soil-survey/soil-mapsand-datab ases/).

We predict the daily carbon flux in the 78 forest sites and then validate the predictions with the

observations. As the overall performance, **Fig. 2** shows the direct daily comparison between predictions

and observations. Overall, the model had the best performance in capturing GPP dynamics, followed by

ER and NEP (i.e. the predicted GPP has the highest R). In the FORCCHN2 model, we use the phenology

model and the optimized phenological parameters to predict the leaf growth, which could improve the

predicted performance of GPP (Fang et al. 2020b). We did the statistics for the results in all sites. The

validation statistics include the correlation coefficient (R), model efficiency (E, calculated by **Eqn S60**),

root mean square error ($RMSE$), mean absolute error (MAE), and bias ($Bias$, calculated by **Eqn S61**). The

calculation of each statistic can be found in ***Methods S4***. Each site had one group of statistics. **Fig. 3**

shows that the FORCCHN2 model could reproduce the daily dynamics of the carbon flux in all sites,

particularly for predicting daily GPP (median of all sites: R= 0.86, E=0.62, $RMSE$=2.29 g C m^{-2} d^{-1},

MAE=1.61 g C m^{-2} d^{-1}). The predicted ER performs lower than GPP (i.e. the median of R and E from the

predicted ER is less than GPP) but shows a high correlation with the observed ER (median: R=0.83,

E=0.25, $RMSE$=1.46 g C m^{-2} d^{-1}, MAE=1.04 g C m^{-2} d^{-1}). NEP results had the lowest performance in all

flux variables (median: R=0.61, E=-0.16, $RMSE$=1.91 g C m^{-2} d^{-1}, MAE=1.43 g C m^{-2} d^{-1}). The highest

uncertainty in predicting NEP maybe because of the compounding effect of GPP and ER errors (Balzarolo

et al. 2014). In terms of bias, FORCCHN2 overestimates the GPP and ER (median: $Bias$=0.49 and 0.56

g C m^{-2} d^{-1}, respectively) but slightly underestimates the NEP (median: $Bias$=−0.14 g C m^{-2} d^{-1}). For the

different forest types, the predictions present well in DBF and MF (R=0.84 and 0.57, E=0.53 and 0.64,

respectively), whereas the lowest performance is found in EBF (R=0.61, E=0.31). These results are

consistent with the previous studies: EBF reveals subtle changes in the leaf phenology and thus increases

the difficulty in modeling photosynthesis (i.e., GPP) (Raczka et al. 2013, Yuan et al. 2014, Piao et al.

2019).

5. Applications in the Northern Hemisphere

As a case application on large scale, we predict the carbon dynamics in the Northern Hemisphere forests

during 1980-2016 (spatial resolution: 0.5×0.5 degree). For the Hemisphere, we use the Simple Biosphere

(SiB) model of the International Satellite Land Surface Climatology Project (ISLSCP II) to represent

forest types (**Fig. S1**, https://daac.ornl.gov/ISLSCP_II) (Friedl et al. 2010). The LAI data are extracted

from the Global Land Surface Satellite (GLASS) Product (http://www.glass.umd.edu/Download.html).

The climate data are from the daily analysis of ERA-Interim in the European Centre for Medium-range

Weather Forecasts (ECMWF) dataset (Hersbach et al. 2020). Soil data are taken from the HWSD V1.2.

Fig. 4 reported the spatial distribution of 37-year averaged GPP, above- and belowground autotrophic respiration, soil heterotrophic respiration, net primary productivity (NPP), and net ecosystem productivity (NEP) for forest area. All results show a similar spatial pattern with the largest fluxes occurring around the equator, such as the northern part of the Amazon and Central African tropical rainforests; secondly, the monsoonal subtropical regions such as South Asia and eastern North America show the large fluxes; the northern forests near the Arctic Circle had the smallest fluxes. Overall, our predictions demonstrate that the forests in Northern Hemisphere had a huge carbon sink potential by the vegetation (i.e., NPP=16.76 Pg C year^{-1} or 61.45 Gt CO_2 year^{-1}) and the total ecosystem (NEP=3.19 Pg C year^{-1} or 11.70 Gt CO_2 year^{-1}) during 1980-2016, which is within the range of the newest estimation of forest carbon sinks (Harris et al. 2021). As the comparisons, we use the aboveground biomass (AGB) from the GLASS product (a satellite-derived product, http://www.glass.umd.edu/Download.html) and the carbon fluxes from the FluxCom dataset (https://www.bgc-jena.mpg.de/geodb/projects/Data.php) to test our predictions (**Fig. S2** and **Fig. S3**). Both predictions and GLASS observations present the tropical forests own the highest AGB and the boreal forests had the smallest AGB (**Fig. S2**). In terms of carbon fluxes (i.e. GPP, ER, and NEP), the resulting spatial pattern is consistent with the FluxCom dataset (**Fig. S3**). However, the GPP and ER derived from FORCCHN2 for some boreal forests are approximately 0.5 kg C m^{-2} year^{-1} smaller and for parts of eastern North America are approximately 0.5 kg C m^{-2} year^{-1} larger than those of FluxCom GPP and ER, respectively. Compared to the FluxCom NEP, the model overestimates NEP in

217 some tropical forests and underestimates NEP in some boreal forests.

218 The predicted carbon results including the variables of 'dayout' and 'yearout' in this case (i.e.,

219 Northern Hemisphere forests) are deposited at an open-access repository (Fang 2022:

220 https://doi.org/10.6084/m9.figshare.18318722.v1).

221

222 6. Conclusions

223 We develop the FORCCHN2 model and design the corresponding DLL package with the intention to

224 simplify the input and processing of the model and make it more accessible to ecologists interested in the

225 forest ecosystem, climate change, carbon cycle, and modeling. This package provides convenient access

226 and allows high computational efficiency with the Fortran-language-based model predicting the daily

227 dynamics of individual trees. With this new package, we have demonstrated the workflow, functions, and

228 applications of the FORCCHN2 model.

229 In addition, the FORCCHN2 model is tested at 78 flux sites, and then it is applied in predicting the

230 carbon dynamics in the whole Northern Hemisphere forests (1980-2016). Our assessment indicated that

231 FORCCHN2 is able to predict the satisfactory carbon dynamics. While we provided publicly available

232 data in the Northern Hemisphere with 0.5 degrees, our hope is that end-users can offer a wide range of

233 applications and analyses of the FORCCHN2 model, such as providing the new dataset with finer

234 resolution and estimating future changes of forest carbon fluxes. We are also open to further suggestions

235   on enhanced functions that ecologists may find helpful in the subsequent model versions.

236

237   **Acknowledgements**

238   This study is supported by the National Natural Science Foundation of China (32101349, 32171599).

239   This study also is supported by the Key Program of the National Natural Science Foundation of China

240   (32130069) and the National Key Research and Development Program of China (grant

241   2019YFC0606904).

242

243   **Authors' contributions**

244   JF planned the project. XY and JF conducted the modeling. XY, JF, YS, and FL contributed to data

245   collection. HHS and JF contributed to data analysis and interpretation of the results. HHS, FL and JF took

246   the lead in writing the manuscript. JF feedback and approval from co-authors. The authors have no

247   conflicts of interest to report.

248

249   **Data availability statement**

250   The source code, instructions, and example run, together with FORCCHN2 DLL package are publicly

251   available via https://doi.org/10.5281/zenodo.6351153 (Fang et al. 2022). The datasets predicted by

252   FORCCHN2 model include the 37-year (1980-2016) GPP, above- and belowground autotrophic

253   respiration, soil heterotrophic respiration for Northern Hemisphere forests (0.5º × 0.5º) are publicly

254   available via https://doi.org/10.6084/m9.figshare.18318722.v1 (Fang 2022).

255

Reference

257   Balzarolo, M., S. Boussetta, G. Balsamo, A. Beljaars, F. Maignan, J. C. Calvet, S. Lafont, A. Barbu, B. Poulter, F. Chevallier,
258   C. Szczypta, and D. Papale. 2014. Evaluating the potential of large-scale simulations to predict carbon fluxes
259   of terrestrial ecosystems over a European Eddy Covariance network. Biogeosciences **11**:2661-2678.
260   Beer, C., M. Reichstein, E. Tomelleri, P. Ciais, M. Jung, N. Carvalhais, C. Rödenbeck, M. A. Arain, D. Baldocchi, B. Bonan
261   Gordon, A. Bondeau, A. Cescatti, G. Lasslop, A. Lindroth, M. Lomas, S. Luyssaert, H. Margolis, W. Oleson Keith,
262   O. Roupsard, E. Veenendaal, N. Viovy, C. Williams, F. I. Woodward, and D. Papale. 2010. Terrestrial Gross
263   Carbon Dioxide Uptake: Global Distribution and Covariation with Climate. Science **329**:834-838.
264   Delpierre, N., S. Lireux, F. Hartig, J. J. Camarero, A. Cheaib, K. Čufar, H. Cuny, A. Deslauriers, P. Fonti, J. Gričar, J.-G.
265   Huang, C. Krause, G. Liu, M. de Luis, H. Mäkinen, E. M. del Castillo, H. Morin, P. Nöjd, W. Oberhuber, P. Prislan,
266   S. Rossi, S. M. Saderi, V. Treml, H. Vavrick, and C. B. K. Rathgeber. 2019. Chilling and forcing temperatures
267   interact to predict the onset of wood formation in Northern Hemisphere conifers. Global Change Biology
268   **25**:1089-1105.
269   Fang, J. 2022. Daily and annual carbon flux predicted by FORCCHN2 model. figshare.
270   Fang, J., H. H. Shugart, Liu, F., Yan X., Song, Y., and Lv, F. 2022. FORCCHN2 model (v2.0.1). Zenodo.
271   https://doi.org/10.5281/zenodo.6351153
272   Fang, J., J. A. Lutz, H. H. Shugart, and Yan X. 2020a. A physiological model for predicting dynamics of tree stem-wood
273   non-structural carbohydrates. Journal of Ecology **108**:702-718.
274   Fang, J., J. A. Lutz, H. H. Shugart, Yan X., Xie W., and F. Liu. 2021. Improving intra- and inter-annual GPP predictions
275   by using individual tree inventories and leaf growth dynamics. Journal of Applied Ecology **58**:2315-2328.
276   Fang, J., J. A. Lutz, Wang L., H. H. Shugart, and Yan X. 2020b. Using climate-driven leaf phenology and growth to
277   improve predictions of gross primary productivity in North American forests. Global Change Biology **26**:6974-
278   6988.
279   Fang, J., J. A. Lutz,, H. H. Shugart,, Wang L., Liu F., and Yan X. 2022. Continental-scale parameterization and prediction
280   of leaf phenology for the North American forests. Global Ecology and Biogeography, **00:**1–13.
281   https://doi.org/10.1111/geb.13533
282   Friedl, M. A., A. H. Strahler, and J. Hodges. 2010. ISLSCP II MODIS (Collection 4) IGBP Land Cover, 2000-2001. ORNL
283   Distributed Active Archive Center.
284   Friedlingstein, P., M. O'Sullivan, M. W. Jones, R. M. Andrew, J. Hauck, A. Olsen, G. P. Peters, W. Peters, J. Pongratz, S.
285   Sitch, C. Le Quéré, J. G. Canadell, P. Ciais, R. B. Jackson, S. Alin, L. E. O. C. Aragão, A. Arneth, V. Arora, N. R.

Bates, M. Becker, A. Benoit-Cattin, H. C. Bittig, L. Bopp, S. Bultan, N. Chandra, F. Chevallier, L. P. Chini, W. Evans, L. Florentie, P. M. Forster, T. Gasser, M. Gehlen, D. Gilfillan, T. Gkritzalis, L. Gregor, N. Gruber, I. Harris, K. Hartung, V. Haverd, R. A. Houghton, T. Ilyina, A. K. Jain, E. Joetzjer, K. Kadono, E. Kato, V. Kitidis, J. I. Korsbakken, P. Landschützer, N. Lefèvre, A. Lenton, S. Lienert, Z. Liu, D. Lombardozzi, G. Marland, N. Metzl, D. R. Munro, J. E. M. S. Nabel, S. I. Nakaoka, Y. Niwa, K. O'Brien, T. Ono, P. I. Palmer, D. Pierrot, B. Poulter, L. Resplandy, E. Robertson, C. Rödenbeck, J. Schwinger, R. Séférian, I. Skjelvan, A. J. P. Smith, A. J. Sutton, T. Tanhua, P. P. Tans, H. Tian, B. Tilbrook, G. van der Werf, N. Vuichard, A. P. Walker, R. Wanninkhof, A. J. Watson, D. Willis, A. J. Wiltshire, W. Yuan, X. Yue, and S. Zaehle. 2020. Global Carbon Budget 2020. Earth Syst. Sci. Data **12**:3269-3340.

Furze, M. E., B. A. Huggett, D. M. Aubrecht, C. D. Stolz, M. S. Carbone, and A. D. Richardson. 2019. Whole-tree nonstructural carbohydrate storage and seasonal dynamics in five temperate species. New Phytologist **221**:1466-1477.

Harris, N. L., D. A. Gibbs, A. Baccini, R. A. Birdsey, S. de Bruin, M. Farina, L. Fatoyinbo, M. C. Hansen, M. Herold, R. A. Houghton, P. V. Potapov, D. R. Suarez, R. M. Roman-Cuesta, S. S. Saatchi, C. M. Slay, S. A. Turubanova, and A. Tyukavina. 2021. Global maps of twenty-first century forest carbon fluxes. Nature Climate Change **11**:234-240.

Hersbach, H., B. Bell, P. Berrisford, S. Hirahara, A. Horányi, J. Muñoz-Sabater, J. Nicolas, C. Peubey, R. Radu, D. Schepers, A. Simmons, C. Soci, S. Abdalla, X. Abellan, G. Balsamo, P. Bechtold, G. Biavati, J. Bidlot, M. Bonavita, G. De Chiara, P. Dahlgren, D. Dee, M. Diamantakis, R. Dragani, J. Flemming, R. Forbes, M. Fuentes, A. Geer, L. Haimberger, S. Healy, R. J. Hogan, E. Hólm, M. Janisková, S. Keeley, P. Laloyaux, P. Lopez, C. Lupu, G. Radnoti, P. de Rosnay, I. Rozum, F. Vamborg, S. Villaume, and J.-N. Thépaut. 2020. The ERA5 global reanalysis. Quarterly Journal of the Royal Meteorological Society **146**:1999-2049.

Houlahan, J. E., S. T. McKinney, T. M. Anderson, and B. J. McGill. 2017. The priority of prediction in ecological understanding. Oikos **126**:1-7.

Huntzinger, D. N., W. M. Post, Y. Wei, A. M. Michalak, T. O. West, A. R. Jacobson, I. T. Baker, J. M. Chen, K. J. Davis, D. J. Hayes, F. M. Hoffman, A. K. Jain, S. Liu, A. D. McGuire, R. P. Neilson, C. Potter, B. Poulter, D. Price, B. M. Raczka, H. Q. Tian, P. Thornton, E. Tomelleri, N. Viovy, J. Xiao, W. Yuan, N. Zeng, M. Zhao, and R. Cook. 2012. North American Carbon Program (NACP) regional interim synthesis: Terrestrial biospheric model intercomparison. Ecological Modelling **232**:144-157.

Keenan, T. F., and C. A. Williams. 2018. The Terrestrial Carbon Sink. Annual Review of Environment and Resources **43**:219-243.

Lasslop, G., M. Reichstein, D. Papale, A. D. Richardson, A. Arneth, A. Barr, P. Stoy, and G. Wohlfahrt. 2010. Separation of net ecosystem exchange into assimilation and respiration using a light response curve approach: critical issues and global evaluation. Global Change Biology **16**:187-208.

Ma, J., H. H. Shugart, X. Yan, C. Cao, S. Wu, and J. Fang. 2017. Evaluating carbon fluxes of global forest ecosystems by using an individual tree-based model FORCCHN. Science of The Total Environment **586**:939-951.

Martínez-Vilalta, J., A. Sala, D. Asensio, L. Galiano, G. Hoch, S. Palacio, F. I. Piper, and F. Lloret. 2016. Dynamics of non-structural carbohydrates in terrestrial plants: a global synthesis. Ecological Monographs **86**:495-516.

323 Pan, Y., A. Birdsey Richard, J. Fang, R. Houghton, E. Kauppi Pekka, A. Kurz Werner, L. Phillips Oliver, A. Shvidenko, L.
324   Lewis Simon, G. Canadell Josep, P. Ciais, B. Jackson Robert, W. Pacala Stephen, A. D. McGuire, S. Piao, A.
325   Rautiainen, S. Sitch, and D. Hayes. 2011. A Large and Persistent Carbon Sink in the World's Forests. Science
326   **333**:988-993.

327 Pastorello, G., C. Trotta, E. Canfora, H. Chu, D. Christianson, Y.-W. Cheah, … and D. Papale. 2020. The FLUXNET2015
328   dataset and the ONEFlux processing pipeline for eddy covariance data. Scientific data **7**:225.

329 Piao, S., Q. Liu, A. Chen, I. A. Janssens, Y. Fu, J. Dai, L. Liu, X. Lian, M. Shen, and X. Zhu. 2019. Plant phenology and
330   global climate change: Current progresses and challenges. Global Change Biology **25**:1922-1940.

331 Piper, F. I. 2020. Decoupling between growth rate and storage remobilization in broadleaf temperate tree species.
332   Functional ecology **34**:1180-1192.

333 Raczka, B. M., K. J. Davis, D. Huntzinger, R. P. Neilson, B. Poulter, A. D. Richardson, J. Xiao, I. Baker, P. Ciais, T. F. Keenan,
334   B. Law, W. M. Post, D. Ricciuto, K. Schaefer, H. Tian, E. Tomelleri, H. Verbeeck, and N. Viovy. 2013. Evaluation
335   of continental carbon cycle simulations with North American flux tower observations. Ecological Monographs
336   **83**:531-556.

337 Reichstein, M., E. Falge, D. Baldocchi, D. Papale, M. Aubinet, P. Berbigier, C. Bernhofer, N. Buchmann, T. Gilmanov, A.
338   Granier, T. Grünwald, K. Havránková, H. Ilvesniemi, D. Janous, A. Knohl, T. Laurila, A. Lohila, D. Loustau, G.
339   Matteucci, T. Meyers, F. Miglietta, J.-M. Ourcival, J. Pumpanen, S. Rambal, E. Rotenberg, M. Sanz, J. Tenhunen,
340   G. Seufert, F. Vaccari, T. Vesala, D. Yakir, and R. Valentini. 2005. On the separation of net ecosystem exchange
341   into assimilation and ecosystem respiration: review and improved algorithm. Global Change Biology **11**:1424-
342   1439.

343 Richardson, A. D., M. S. Carbone, T. F. Keenan, C. I. Czimczik, D. Y. Hollinger, P. Murakami, P. G. Schaberg, and X. Xu.
344   2013. Seasonal dynamics and age of stemwood nonstructural carbohydrates in temperate forest trees. New
345   Phytologist **197**:850-861.

346 Sala, A., D. R. Woodruff, and F. C. Meinzer. 2012. Carbon dynamics in trees: feast or famine? Tree physiology **32**:764-
347   775.

348 Schiestl-Aalto, P., L. Kulmala, H. Mäkinen, E. Nikinmaa, and A. Mäkelä. 2015. CASSIA – a dynamic model for predicting
349   intra-annual sink demand and interannual growth variation in Scots pine. New Phytologist **206**:647-659.

350 Yuan, W., W. Cai, J. Xia, J. Chen, S. Liu, W. Dong, L. Merbold, B. Law, A. Arain, J. Beringer, C. Bernhofer, A. Black, P. D.
351   Blanken, A. Cescatti, Y. Chen, L. Francois, D. Gianelle, I. A. Janssens, M. Jung, T. Kato, G. Kiely, D. Liu, B. Marcolla,
352   L. Montagnani, A. Raschi, O. Roupsard, A. Varlagin, and G. Wohlfahrt. 2014. Global comparison of light use
353   efficiency models for simulating terrestrial vegetation gross primary production based on the LaThuile
354   database. Agricultural and Forest Meteorology **192-193**:108-120.

355 Zhao, J., J. Ma, and Y. Zhu. 2019. Evaluating impacts of climate change on net ecosystem productivity (NEP) of global
356   different forest types based on an individual tree-based model FORCCHN and remote sensing. Global and
357   Planetary Change **182**:103010.

Table 1. Description of functions and variables in the FORCCHN2 model. A detailed explanation of functions and variables can be found in the FORCCHN2 DLL package documentation. SOS: the start time of leaf growth; EOS: the end time of leaf growth; DOY: day of the year; GPP: gross primary productivity.

Model functions and variables	Description
Time step	Daily and yearly
Initialization data (inputs)	**Vegetation:** maximum LAI (m^2 m^{-2}), forest types, SOS dates (DOY), EOS dates (DOY) **Soil:** field capacity (cm), permanent wilting point (cm), soil volume weight (kg m^{-3}), total organic carbon (kg C m^{-2}), total nitrogen (kg C m^{-2}), silt percent (%), sand percent (%) **Geography:** latitude (°), longitude (°), elevation (m)
Driven data (inputs)	**Daily climate:** Mean temperature (°C), maximum temperature (°C), minimum temperature (°C), air pressure (hPa), wind (m s^{-1}), relative humidity (%), precipitation (mm), shortwave radiation (W m^{-2}), CO_2 concentration (ppm)

Outputs	**Daily:** aboveground vegetation biomass (kg C m^{-2}), belowground vegetation biomass (kg C m^{-2}), GPP (kg C m^{-2}), aboveground autotrophic respiration (kg C m^{-2}), belowground autotrophic respiration (kg C m^{-2}), soil heterotrophic respiration (kg C m^{-2}), litter-fall (kg C m^{-2}), soil total organic carbon (kg C m^{-2}) **Yearly:** same as the daily outputs, with the SOS dates (DOY) and EOS dates (DOY)
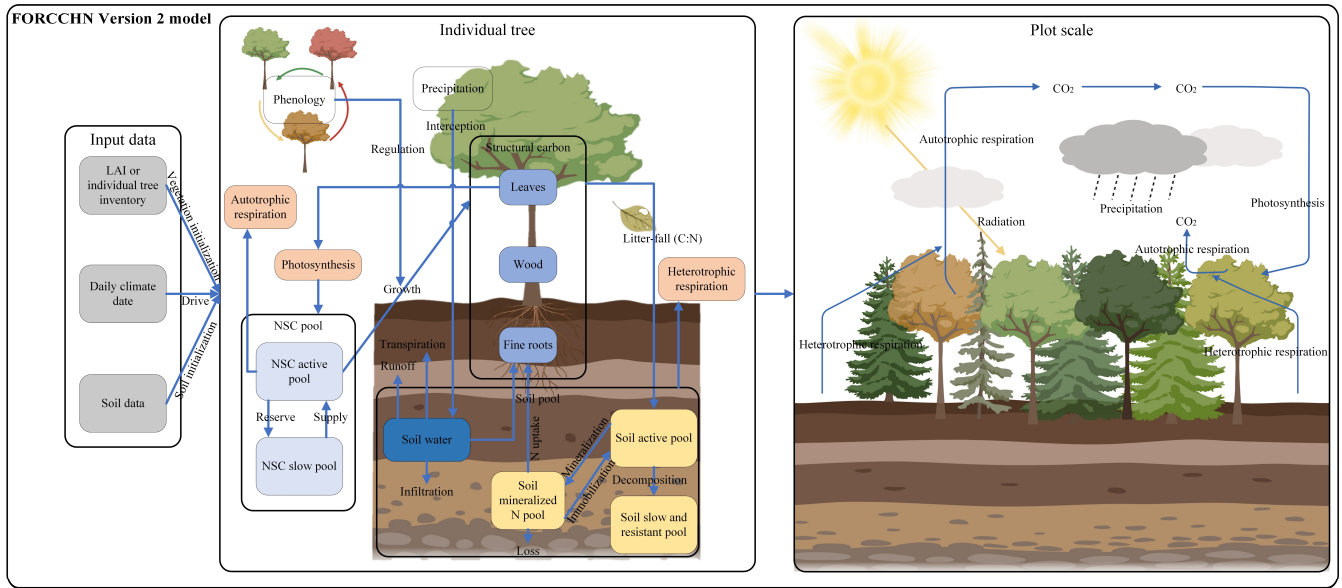
Fig. 1. Schematic representation of the FORCCHN2 model. LAI: leaf area index; NSC: non-structural carbohydrates; C: carbon; N: nitrogen.
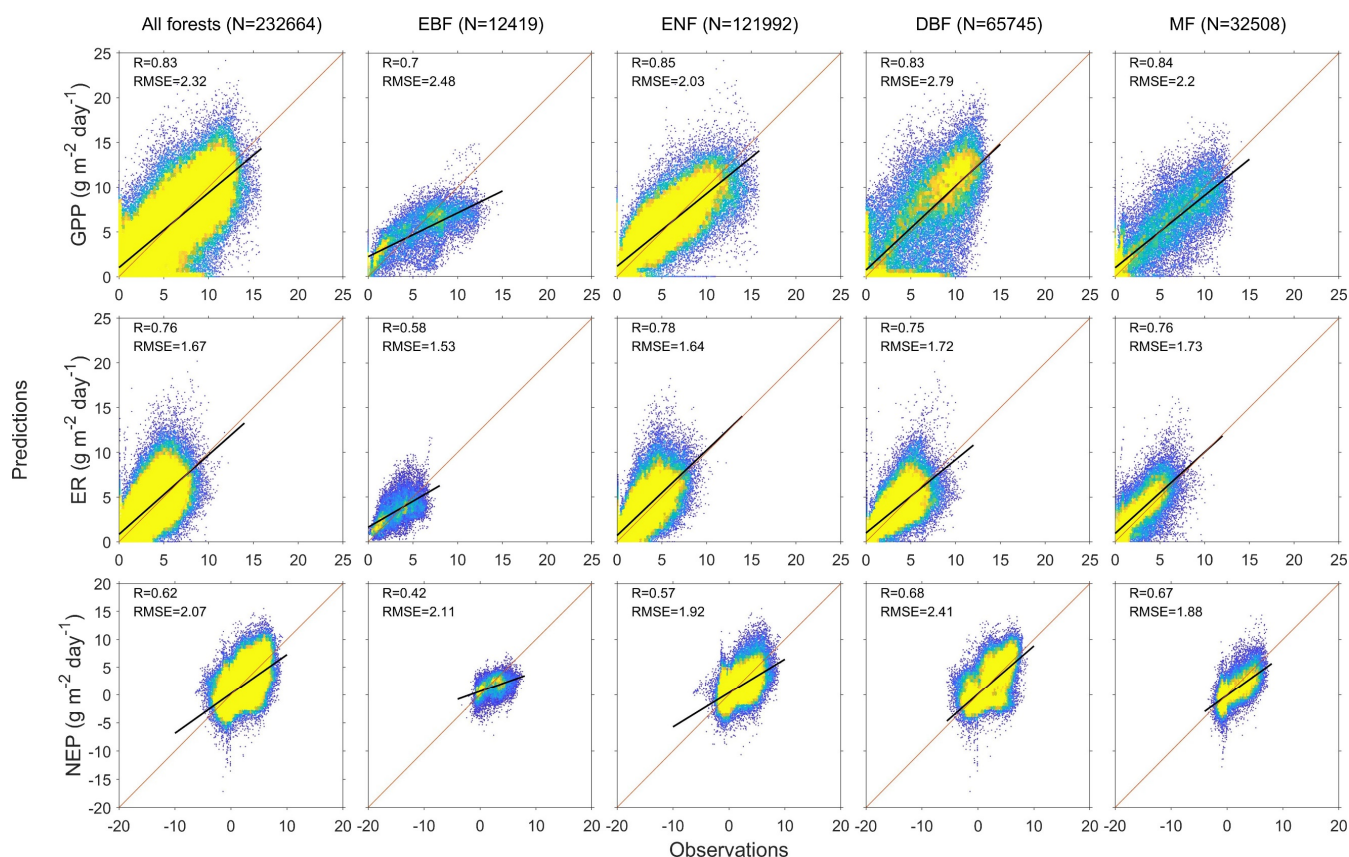
Fig.2. Heat plots showing the relationship between predictions and observations of daily gross primary productivity (GPP), ecosystem respiration (ER), and net ecosystem productivity (NEP) of the studied EC sites. N: the total days of all sites; R: correlation coefficient; RMSE: root mean square error (unit: g C m^{-2} day^{-1}). EBF: evergreen broadleaf forest; ENF: evergreen needleleaf forest; DBF: deciduous broadleaf forest; MF: mixed forest. Diagonal lines are 1:1 lines, indicating perfect agreement between predicted and observed fluxes. Black lines represent the linear regression. Colors indicate the percentage of pixels in each bin area (yellow is the densest).
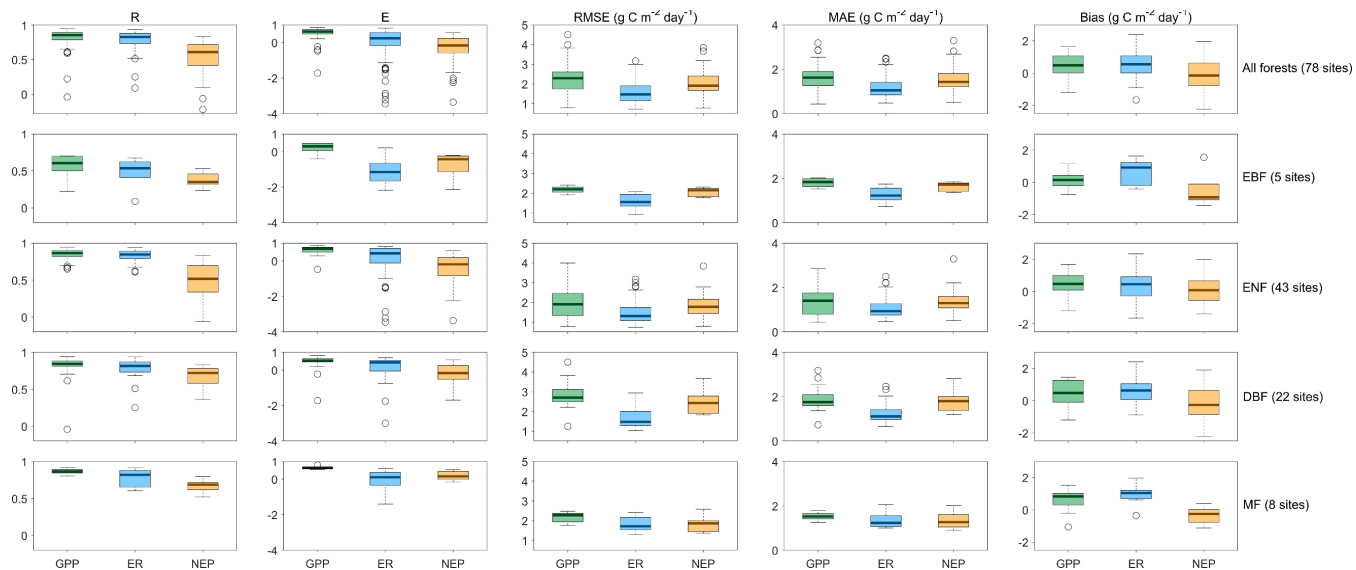
Fig. 3. The statistical results of daily gross primary productivity (GPP, green), ecosystem respiration (ER, blue), and net ecosystem productivity (NEP, tan) observations versus predictions in the studied EC sites. R: correlation coefficient; E: model efficiency; RMSE: root mean square error; MAE: mean absolute error; Bias: bias. EBF: evergreen broadleaf forest; ENF: evergreen needleleaf forest; DBF: deciduous broadleaf forest; MF: mixed forest.
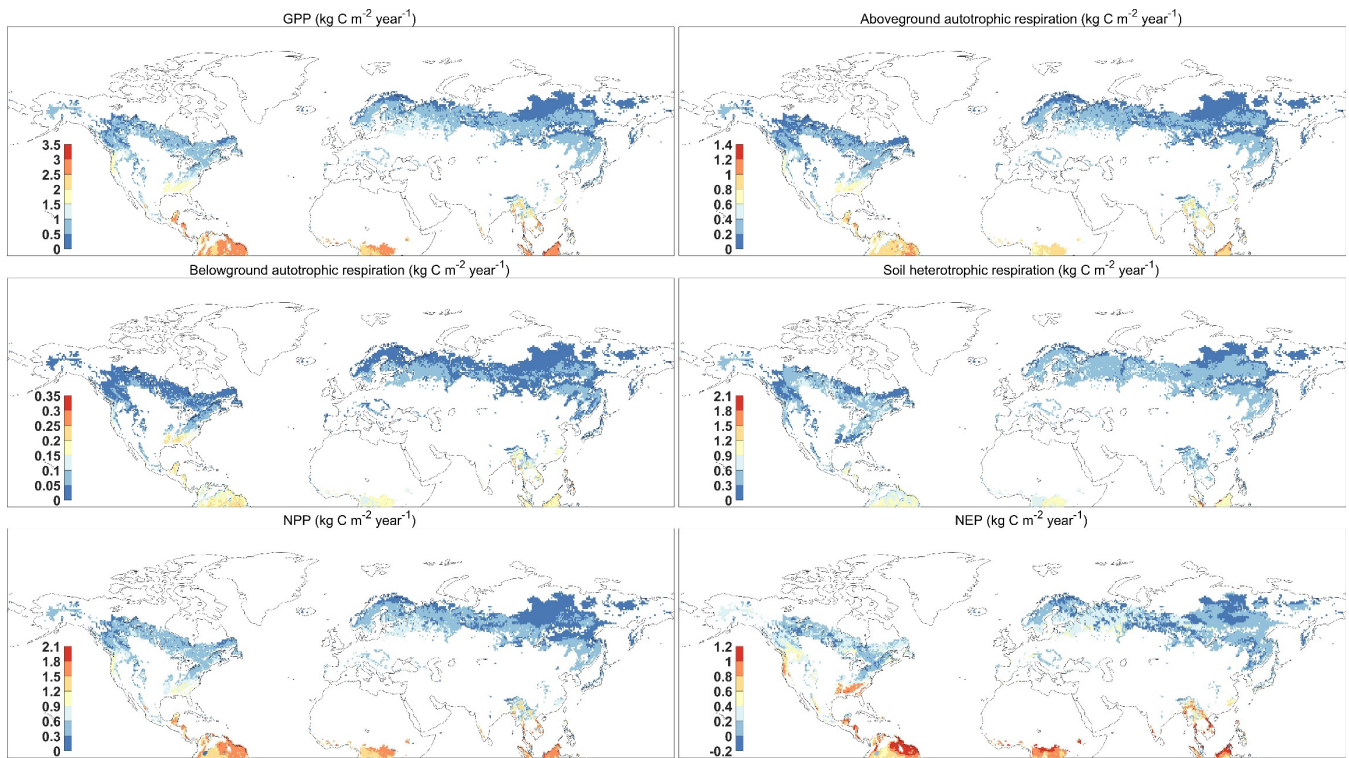
Fig. 4. The spatial distribution of mean GPP (Gross Primary Productivity), above- and belowground autotrophic respiration, soil heterotrophic respiration, NPP (Net Primary Productivity), and NEP (Net Ecosystem Productivity) predicted by the FORCCHN2 model for forest ecosystems of the Northern Hemisphere during 1980–2016. The spatial resolution is 0.5º×0.5º.